Circ-CTNNB1 Drives Aerobic Glycolysis and Osteosarcoma Progression via m6A Modification Through Interacting With RBM15

Hucheng Liu
First Affiliated Hospital of Nanchang University
Jun Xiao
First Affiliated Hospital of Nanchang University
Bo Li
First Affiliated Hospital of Nanchang University
Yajun Chen
Huazhong University of Science and Technology Tongji Medical College
Jin Zeng
First Affiliated Hospital of Nanchang University
Anpei Hu
Huazhong University of Science and Technology Tongji Medical College
Song Zhou
First Affiliated Hospital of Nanchang University
Yangyang Liu
The First Affiliated Hospital of Nanchang University
Feng Yang (D201781340@hust.edu.cn)
First Affiliated Hospital of Nanchang University

Research

Keywords: Circ-CTNNB1, RNA binding motif protein 15, N6-methyladenosine, Aerobic glycolysis, Osteosarcoma

Posted Date: November 8th, 2021

DOI: https://doi.org/10.21203/rs.3.rs-991482/v1

Abstract

Background

In a previous study, we have identified that circ-CTNNB1 (a circular RNA derived from CTNNB1) drives cancer progression through the activation of the Wnt/β-catenin signaling pathway in various tumors. However, the functions of circ-CTNNB1 in regulating osteosarcoma (OS, a highly malignant bone tumor in children and adolescents) remain unclear. In this study, we aimed to assess the role of circ-CTNNB1 in OS and identify the underlying mechanisms, which may contribute to the exploration of a potential therapeutic strategy for OS.

Methods

Circ-CTNNB1 was analyzed by qRT-PCR, and the results were confirmed by Sanger sequencing. The interaction and effects between circ-CTNNB1 and RNA binding motif protein 15 (RBM15) were analyzed through biotin-labeled RNA pull-down and mass spectrometry, in vitro binding, and RNA electrophoretic mobility shift assays. In vitro and in vivo experiments were performed to evaluate the biological functions and underlying mechanisms of circ-CTNNB1 and RBM15 in OS cells.

Results

Circ-CTNNB1 was highly expressed in OS tissues and predominantly detected in the nucleus of OS cells. Ectopic expression of circ-CTNNB1 promoted the growth, invasion, and metastasis of OS cells in vitro and in vivo. Mechanistically, circ-CTNNB1 interacted with RBM15 and subsequently promoted the expression of hexokinase 2 (HK2), glucose-6-phosphate isomerase (GPI), and phosphoglycerate kinase 1 (PGK1) through N6-methyladenosine (m6A) modification to facilitate the glycolysis process and activate OS progression.

Conclusions

These results indicate that oncogenic circ-CTNNB1 drives aerobic glycolysis and OS progression by facilitating RBM15-mediated m6A modification.

Background

Osteosarcoma (OS) is the most common primary bone malignancy worldwide and mainly occurs in children and adolescents (1–4). Although mutations involved in genes encoding various oncogenic and tumor suppressor proteins play a crucial pathogenic role in OS, it has now been revealed that the dysregulation of non-coding RNAs (ncRNAs), such as circular RNAs (circRNAs), microRNAs (miRNAs), and long non-coding RNAs (lncRNAs), is comparably important to the development of OS (5).

CircRNAs are a group of transcripts characterized by covalently closed continuous loops, primarily produced from pre-mRNAs via non-canonical back-splicing (6, 7). CircRNAs have various functions, including the adsorption of miRNAs or proteins as sponges, interaction with RNA-binding proteins (RBPs), regulation of transcription or alternative splicing, and templates for translation (8–10). Dysregulation of circRNAs has been implicated in various kinds of cancer by promoting or suppressing tumors in different aspects from cancer initiation, proliferation, apoptosis, metastasis, and invasion to treatment resistance (11–15).

Our previous study has demonstrated that circ-CTNNB1, derived from its parent gene β-catenin (CTNNB1), is upregulated in various cancer tissues and associated with a poor outcome of patients. Mechanistically, circ-CTNNB1 binds DEAD-box polypeptide 3 (DDX3) to facilitate its physical interaction with Yin Yang 1 (YY1), which results in the transactivation of YY1 and the subsequent transcriptional alteration of downstream genes associated with cancer progression through β-catenin activation. However, the function of circ-CTNNB1 in regulating OS remains unclear (16).

N6-methyladenosine (m6A), which results from the methylation of adenosine at the N6 position, has been reported to play vital roles in cancer biology (17, 18). The biological effects of m6A are mainly regulated by three kinds of methylation modulators, namely methylation transferases (Writers), demethylases (Erasers), and methylated readers (Readers), based on which the m6A modification is involved in regulating gene expression, splicing, RNA editing, and RNA stability and controlling mRNA life and degradation to participate in the progression of cancers (18–20). In contrast, accumulating evidence has demonstrated that some methylation modulators are regulated by various circRNAs (19, 21). For example, circ_KIAA1429 could maintain the expression of Zeb1 in a YTHDF3 (a m6A reader protein)-dependent manner to accelerate the progression of liver cancer (19). The circMAP2K4/miR-139-5p/YTHDF1 axis, which involves the proliferation of cancer cells, further confirmed the role of circRNAs in regulating m6A RNA methylation modulators (21).

In this study, we detected high expression of circ-CTNNB1 in OS tissues and cell lines, which was associated with lung metastasis in OS patients and malignant progression of OS cells in vitro and in vivo. Mechanistically, circ-CTNNB1 interacts with m6A regulator RBM15, which facilitates the ability of the latter to elevate the m6A levels at the 3’-UTR of the key aerobic glycolysis genes hexokinase 2 (HK2), glucose-6-phosphate isomerase (GPI), and phosphoglycerate kinase 1 (PGK1), ensuring a more stable activity of the target genes. Therefore, OS cells are able to obtain metabolic survival advantage from aerobic glycolysis via the upregulation of circ-CTNNB1.

Materials And Methods

Clinical samples and cell culture

Human samples of osteochondroma (n=20) and OS tissues (n=20) were collected from patients who underwent surgery at the Department of Orthopedic Surgery, The First Affiliated Hospital of Nanchang University (Nanchang, China), and patients have received no preoperative treatment prior to the sample

collection. All procedures were approved by the Ethics Committee of The First Affiliated Hospital of Nanchang University and carried out in accordance with the Helsinki Principles. Written informed consent was provided by all patients. Fresh human samples validated by pathological diagnosis were frozen in liquid nitrogen and stored at −80 °C until RNA extraction. The human osteosarcoma cell lines 143B, HOS, MG-63, SJSA-1, Saos-2, and U2OS and non-tumor control cell line hFOB 1.19 were cultured in DMEM supplemented with 10% fetal bovine serum (FBS).

Real-time PCR and quantitative real-time PCR

Genomic DNA (gDNA) was extracted using the DNA Mini Kit (QIAGEN, Germany). Total RNA was isolated from OS cell lines and tissues using the RNeasy Mini Kit (QIAGEN, Germany) according to the manufacturer's instructions. For the detection of circRNA, RNA samples were treated with RNase R (3 U/ug, Epicenter, Madison, WI, USA) at 37 °C for 15 min, and cDNA was synthesized using the reverse transcription kit (Takara, Japan). Quantification of mRNA, circRNA, and gDNA was performed using the SYBR Green PCR Kit (Takara, Japan) and analyzed by a Real-Time PCR System (Applied Biosystems, USA). The differences of circRNA and mRNA were normalized to the levels of b-actin, and primers are shown in the Additional file 1: Table S1.

Northern blot

The junction probe for circ-CTNNB1 was synthesized and labeled with digoxigenin, as described in our previous study (16). Briefly, 20 μg of total RNA was separated on 3-(N-morpholino) propanesulfonic acid (MOPS)-buffered 2% (w/v) agarose gel containing 1.2% (v/v) formaldehyde under denaturing conditions for 4 h at 80 V and transferred to Hybond-N+ membrane. Prehybridization was carried out at 65 °C for 30 min in DIG Easy Hyb solution (Roche). Hybridizations were performed at 65 °C for 16-18 h. Blots were washed thoroughly, detected by anti-digoxigenin (DIG) antibody staining, and recorded on X-ray films with the chemiluminescence substrate CSPD (Roche).

Western blot

Total proteins from cells were extracted with RIPA lysis buffer (Thermo Scientific, USA). Western blot analysis was performed as described before with antibodies specific for β-actin (ab125402), β-catenin (ab32572), RBM15 (ab244374), ENO1 (ab155102), GPI (ab66340), PGK1 (ab38007), Flag (ab45766, Abcam, USA), ALDOA (sc-390733), and IGF2BP1 (sc-166344, Santa Cruz Biotechnology, USA).

Plasmid construction and stable transfection

Mature linear circ-CTNNB1 (hsa_circ_0123778) was synthesized by TsingKe Biotech Company (Wuhan, China) and inserted into pLCDH-ciR vector (Geenseed Biotech, China), which contained a front circular frame and a back circular frame. Human RBM15 cDNA (2934 bp) was synthesized by TsingKe Biotech Company (Wuhan, China), and the truncations of RBM15 were obtained by PCR amplification with differential primer pairs (Additional file 1: Table S2) and subcloned into pCMV-3Tag-1A (Addgene, Cambridge, USA). Oligonucleotides specific for shRNAs against circ-CTNNB1 or RBM15 (Additional file 1:

Table S2) were inserted into GV298 (Genechem Co., Ltd., Shanghai, China). Lentiviral plasmids were co-transfected with the packaging plasmids psPAX2 and pMD2G into HEK-293T cells. Infectious lentiviruses harvested from cultured cells were processed by ultracentrifugation (2 h at 120,000 g). Stable cell lines were obtained, followed by selection with 2 μg/mL puromycin for 2-3 weeks.

RNA fluorescence in situ hybridization (RNA-FISH)

A biotin-labeled antisense probe for the circ-CTNNB1 junction sequence and probes for GAPDH and U1 were synthesized as we previously described (16). The probes were hybridized using the Fluorescent In Situ Hybridization kit (RiboBio) following the manufacturer's instructions. The nuclei of OS cells were counterstained with 4',6-diamidino-2-phenylindole (DAPI), and the images were analyzed using a Nikon A1Si Laser Scanning Confocal Microscope (Nikon, Japan).

Dual-luciferase reporter assay

The TOP-FLASH and FOP-FLASH reporters for the activity of the canonical Wnt pathway were obtained from Millipore (Temecula, CA, USA). The promoter fragments of human HK2 (-1813/+424), GPI (-1,854/+247), PGK1 (-882/+246), and 3'-UTR of target genes amplified from genomic DNA (Additional file 1: Table S2) were subcloned into pGL3-basic and psiCHECK2. Mutations of m6A sites at the 3'-UTR were performed with the GeneTailor^{TM} Site-Directed Mutagenesis System (Invitrogen). The dual-luciferase assay was performed according to the manufacturer's instructions (Promega). The luciferase signal in the promoter activity assay was normalized to the firefly/Renilla ratio, while the activity of the 3'-UTR reporter was measured by the Renilla/firefly ratio.

Biotin-labeled RNA pull down and mass spectrometry analysis

The biotin-labeled RNA probe for circ-CTNNB1 was in vitro transcribed using the Biotin RNA Labeling Mix kit (Roche) and T7 RNA polymerase, as described in our previous study (22). RNA pull-down assay was performed at room temperature, and the biotinylated proteins were detected by mass spectrometry at the Wuhan Institute of Biotechnology (Wuhan, China).

Fluorescence immunocytochemical staining

OS cells were grown on coverslips, incubated with 5% milk for 1 h, and treated with antibody specific for RBM15 (ab244374, Abcam, USA) at 4 °C overnight. Then, the cells were stained with Alexa Fluor 594 IgG and DAPI. The images were photographed under a Nikon A1Si Laser Scanning Confocal Microscope (Niko, Japan).

Aerobic glycolysis and seahorse extracellular flux assays

Cellular Aerobic glycolysis activity and glucose uptake, lactate production, and adenosine triphosphate (ATP) levels were detected as previously described (22). Extracellular acidification rate and oxygen consumption rate (ECAR, OCR) were measured in response to glucose (10 mM), oligomycin (2 uM), and 2-

deoxyglucose (2-DG, 100 mM) under basal conditions with a Seahorse Biosciences XFe24 Flux Analyzer (North Billerica, MA).

Cross-linking RIP assay

Cells were ultraviolet light cross-linked at 254 nm (200 J/cm^2) in PBS and collected by scraping, and RNA immunoprecipitation (RIP) assay was performed according to the instructions of Magna RIPTM Kit (Millipore), with antibodies specific for RBM15 (ab244374, Abcam, USA), and IGF2BP1 (sc-166344, Santa Cruz Biotechnology, USA). Co-precipitated RNAs were detected by RT-PCR or real-time quantitative PCR with specific primers (Additional file 1: Table S1).

In vitro binding assay

Five truncates of RBM15 were cloned with primers (Additional file 1: Table S1) into vectors with flag tag as we described previously (23). The Flag-RBM15 and circ-CTNNB1 complexes were pulled down using Flag beads (Sigma, USA). Circ-CTNNB1 was measured by RT-PCR with divergent primers (Additional file 1: Table S1), and protein was validated by western blot.

RNA electrophoretic mobility shift assay (EMSA)

Biotin-labeled circ-CTNNB1 probe was prepared as described above. RNA EMSA was conducted according to the instructions of LightShift Chemiluminescent RNA EMSA Kit (Thermo Fisher Scientific, Inc.)

In vitro cell viability, growth, and invasion assays

The in vitro viability, growth, and invasion capabilities of OS cells were detected by MTT colorimetry, colony formation, and matrigel invasion assays, as described previously (24).

Xenografts in mice

Circ-CTNNB1 knockdown frame was inserted into GV298 vector (Genechem Co., Ltd., Shanghai, China), and the expression of the mCherry fluorescent protein was detected and imaged by the In-Vivo Xtreme II small animal imaging system (Bruker Corporation, Billerica, MA, USA). For in vivo tumor growth studies, MG-63 cells (1×10^7) were subcutaneously injected into the dorsal flanks of five-week-old male BALB/c nude mice (n=5 per group) in a blind, randomized fashion. The growth and weight of xenografts were detected one month later. In experimental metastasis studies, tail vein injection of MG-63 (5×10^6) cells was performed in a blind, randomized fashion in five-week-old male BALB/c nude mice (n=5 per group). Metastasis counts and survival time of each mouse were monitored and recorded, and the xenografts were studied by hematoxylin and eosin (H&E) and IHC staining. All animal experiments were performed in accordance with the NIH Guidelines for the Care and Use of Laboratory Animals and approved by the Animal Care Committee of Tongji Medical College.

Statistical Analysis

All data are presented as the mean ± standard error of the mean (SEM) processed by GraphPad Prism 5.0 (La Jolla, USA). Student's t-test or one-way analysis of variance (one-way ANOVA) was used to evaluate differences between groups. All statistical tests were two sided. A value of $P < 0.05$ was considered statistically significant.

Results

Circ-CTNNB1 is upregulated in human OS tissues and cells

In a previous study, we identified that circ-CTNNB1 drives cancer growth, invasion, and metastasis through the activation of β-catenin in several cancer models, including gastric cancer, colon cancer, and prostate cancer, while no further studies have been conducted on this circRNA in OS to date. The generation of circ-CTNNB1 from CTNNB1 was first analyzed by RT-PCR with divergent primers, and Sanger sequencing confirmed the predicted back-splicing junction in OS cells (Fig. 1a). Furthermore, using divergent primers of circ-CTNNB1, PCR products could only be amplified from cDNA but not from genomic DNA in 143B and MG-63 cells (Fig. 1b). Circ-CTNNB1 was resistant to RNase R digestion, while the linear RNA of CTNNB1 was significantly reduced after RNase R treatment in 143B and MG-63 cells (Fig. 1c). Higher endogenous expression levels of circ-CTNNB1 were observed in OS cells than those of hFOB 1.19 cells in qRT-PCR assay (Fig. 1d) and Northern blot assay using total RNA extracted from cell lines with a junction-specific probe (Fig. 1e). Moreover, we detected the expression profiles in samples of clinical patients with ten paired osteochondroma and OS tissues by qRT-PCR, revealing that circ-CTNNB1 was upregulated in the OS tissues, and high circ-CTNNB1 expression was associated with lung metastasis in OS patients (Fig. 1f). Subcellular fractionation and RNA fluorescence in situ hybridization (FISH) assays indicated the nuclear enrichment of circ-CTNNB1 in 143B and MG-63 cells (Fig. 1g; Additional file 2: Fig. S1a). To investigate the cis-acting properties of circ-CTNNB1 in regulating β-catenin signaling, overexpression or knockdown of circ-CTNNB1 in OS cells was estabilshed (Additional file 2: Fig. S1b, c). The TOP/FOP flash assay revealed that neither ectopic expression nor knockdown of circ-CTNNB1 affected the RNA transcripts, protein expression, or β-catenin activity in 143B and MG-63 cells (Additional file 2: S1c, Fig. 1h, i). These results demonstrated a relatively higher expression of circ-CTNNB1 in OS tissues and cells.

Circ-CTNNB1 exerts an oncogenic role in OS progression in vitro and in vivo

To explore the roles of circ-CTNNB1 in OS progression, the impacts on the tumorigenesis and aggressiveness were investigated in 143B and MG-63 cells with stable transfection of two independent shRNAs against circ-CTNNB1. In MTT colorimetric assay, stable knockdown of circ-CTNNB1 decreased the vitality of OS cells, than those stably transfected with scramble shRNA (sh-Scb) (Fig. 2a). In colony formation and matrigel invasion assays, stable knockdown of circ-CTNNB1 reduced the growth and invasion capability of 143B and MG-63 cells (Fig. 2b, c). Consistently, stable transfection of sh-circ-CTNNB1 resulted in a significant inhibition in the tumor growth of xenografts formed

by subcutaneous injection of MG-63 cells into athymic nude mice (Fig. 2d, e). Importantly, in the experimental metastasis assay, nude mice treated with tail vein injection of MG-63 cells with stable knockdown of circ-CTNNB1 displayed statistically less lung metastatic colonies and a greater survival probability than the control group (Fig. 2f-h). Taken together, these results showed that silencing circ-CTNNB1 inhibits the growth and aggressiveness of OS cells in vitro and in vivo.

Circ-CTNNB1 directly interacts with m6A regulator RBM15

Previous studies have shown that circRNA can regulate cancer progression through binding with RNA binding proteins. Given the nuclear location of circ-CTNNB1, we hypothesized that circ-CTNNB1 may regulate OS progression via potential protein partners. To evidence our hypothesis, we performed a proteomic analysis of circ-CTNNB1-associated proteins in MG-63 cells by the RNA pull-down assay with a biotin-labeled probe, as described before (16). The mass spectrometry (MS) assay revealed 89 differential proteins of circ-CTNNB1 pull-down from MG-63 cells and overlapping with the critical m6A regulators (25) and differentially expressed genes between OS and normal tissues in GSE87624, indicating two potential circ-CTNNB1-interacting partners (Fig. 3a). Furthermore, RNA immunoprecipitation (RIP) assay validated the interaction of circ-CTNNB1 with the m6A writer RNA binding motif protein 15 (RBM15) but not with insulin-like growth factor 2 mRNA-binding protein 1 (IGF2BP1) in OS cells (Fig. 3b). Moreover, transfection of circ-CTNNB1 increased its enrichment in RNA co-precipitated by RBM15 antibody in MG-63 cells (Fig. 3c). Dual RNA-FISH and immunofluorescence assays confirmed the nuclear colocalization of circ-CTNNB1 and RBM15 in 143B and MG-63 cells (Fig. 3d). Consistently, the RNA electrophoretic mobility shift assay (EMSA) showed that circ-CTNNB1 interacted strongly with endogenous RBM15 in nuclear extracts (Fig. 3e). We further investigated the interaction domain between circ-CTNNB1 and RBM15. The in vitro binding assay indicated that the RBM15 domain (374-451 amino acids), but not other domains of FLAG-tagged RBM15 protein, was crucial for the interaction of RBM15 with circ-CTNNB1 (Fig. 3f). These results indicated that circ-CTNNB1 interacted with RBM15.

Circ-CTNNB1 promotes aerobic glycolysis in OS

Aerobic glycolysis is a hallmark of metabolic reprogramming in various cancers. However, the mechanisms regulating the glycolytic activity remain elusive in OS, which is the most common malignant bone tumor in childhood and adolescence. Herein, aerobic glycolysis and seahorse extracellular flux assays were conducted to explore the roles of circ-CTNNB1 in OS. Knockdown of circ-CTNNB1 attenuated the extracellular acidification rate (ECAR) and increased the oxygen consumption rate (OCR) in MG-63 cells, while ectopic expression of circ-CTNNB1 significantly promoted the glycolytic process (Fig. 4a, b; Additional file 2: Fig. S2a, b). Accordingly, knockdown or overexpression of circ-CTNNB1 decreased and increased the glucose uptake, lactate production, and ATP levels of OS cells, respectively (Fig. 4c-e; Additional file 2: Fig. S2c-e). Treatment with 2-deoxyglucose (2-DG), an established glycolysis inhibitor, abolished the increase in these features of MG-63 cells induced by circ-CTNNB1 overexpression in the glucose uptake, lactate production, and ATP levels. Given the nuclear interaction described above, we

investigated the potential effects of circ-CTNNB1 binding with RBM15 in the aerobic glycolysis in OS. Five crucial glycolytic genes were identified as targets of the circ-CTNNB1/RBM15 axis by the comprehensive analysis of RBM15 ClIP-seq and glycolytic genes (Fig. 4f). Notably, ectopic expression or knockdown of RBM15 and circ-CTNNB1 increased and decreased, respectively, the transcripts and protein levels of glucose-6-phosphate isomerase (GPI), hexokinase 2 (HK2), and phosphoglycerate kinase 1 (PGK1), but not of fructose-bisphosphate A (ALDOA) or enolase 1 (ENO1), in OS cells (Fig. 4g-i). These findings indicated that circ-CTNNB1 promotes aerobic glycolysis in OS cells.

Circ-CTNNB1 facilitates RBM15-mediated gene activation via m6A regulation

We further investigated the effects of the interplay and the underlying mechanisms between circ-CTNNB1 and RBM15 on the reguation of the expression of target genes (GPI, HK2, and PGK1) and cancer progression in OS cells. As m6A modification is involved in the post-transcriptional control of gene expression, the mRNA-stabilizing function was tested. Ectopic expression of circ-CTNNB1 and RBM15 promoted the mRNA half-life of target genes in OS cells (Additional file 2: Fig. S3a). Notably, the stable ectopic expression of circ-CTNNB1 abolished the decrease of the half-life, transcript, and protein levels of GPI, HK2, and PGK1 by knockdown of RBM15 in 143B and MG-63 cells (Fig. 5a-c; Additional file 2: Fig. S3a, b). While, neither ectopic expression nor knockdown of RBM15, could affect the promoter activity of GPI, HK2, and PGK1 in 143B and MG-63 cells in the dual-luciferase assay (Additional file 2: S3c, d). Next, the RNA methylation quantification assay was used to analyze whether circ-CTNNB1 and RBM15 regulate target gene expression in a m6A-dependent manner. As expected, the MeRIP-qPCR assay showed that the 3’-UTR of GPI, HK2, and PGK1 was effectively enriched by m6A-specific antibody, and enriched 3’-UTR was remarkably increased in circ-CTNNB1-overexpression cells, which were prevented by knockdown of RBM15 (Fig. 5d). Therefore, we supposed that circ-CTNNB1 could regulate the m6A levels of GPI, HK2, and PGK1. The m6A modification was at the 3’-UTR of the target gene, and several m6A sites were predicted with high confidence by SRAMP (http://www.cuilab.cn/sramp). In the dual-luciferase assay with a reporter containing the 3’-UTR of GPI, HK2, and PGK1, ectopic expression or interference of circ-CTNNB1 and RBM15 promoted and attenuated the 3’-UTR activity in OS cells, respectively (Fig. 5e, f). Importantly, stable overexpression of circ-CTNNB1 increased the wild type 3’-UTR activity, which was reduced by stable knockdown of RBM15, while the luciferase activity of mutated 3’-UTR was not affected in OS cells (Fig. 5g). These results showed that circ-CTNNB1 facilitated RBM5-mediated GPI, HK2, and PGK1 activation via m6A modification.

Circ-CTNNB1 promotes aerobic glycolysis and OS progression by interaction with RBM15

Next, the effects of the interplay of circ-CTNNB1 and RBM15 in OS cells were analyzed. The ectopic expression of circ-CTNNB1 promoted the extracellular acidification rate (ECAR) and reduced the oxygen consumption rate (OCR) in OS cells, which were prevented by knockdown of RBM15 (Fig. 6a, b). Accordingly, stable interference of RBM15 abolished the increase of the glucose uptake, lactate production, and ATP levels induced by circ-CTNNB1 overexpression in 143B and MG-63 cells (Fig. 6c-

e). Notably, stable circ-CTNNB1 overexpression was facilitated, and MTT, colony formation, and matrigel invasion assays showed the viability, growth, and invasiveness of 143B and MG-63 cells, which were abolished by the knockdown of RBM15, respectively (Fig. 6f-h). Taken together, these results showed that circRNA facilitated the aerobic glycolysis process and OS progression through the circ-CTNNB1/RBM15/m6A axis (Fig. 7).

Discussion

In cancer, circRNAs have the crucial role of acting as miRNA sponge to regulate the miRNA-mRNA axis, thereby driving or suppressing the initiation and progression of cancer, which has been studied extensively (20, 26). Moreover, circRNAs are also able to recruit or sponge proteins, including RBPs, transcription factors, DNA demethylase, and DNA methyltransferase, to the specific regions of target genes or prevent their interaction to regulate transcription and splicing (13). Our previous study demonstrated the essential roles of the circ-CTNNB1/DDX3/YY1 axis in cancer progression. Circ-CTNNB1 promotes β-catenin activation, growth, invasion, and metastasis in virous cancer cells via binding DDX3 to facilitate the physical interaction of the latter with transcription factor YY1, resulting in the transactivation of YY1 and transcriptional alteration of downstream genes associated with β-catenin activation and cancer progression (16). We also found that circ-HuR interacted with CCHC-type zinc finger nucleic acid binding protein (CNBP) and subsequently restrained its binding to the HuR promoter, resulting in the down-regulation of HuR and repression of tumor progression (27).

RBM15 is a member of the SPEN (Split-end) family of proteins. As an RBP, RBM15 binds to RNA by interacting with spliceosome components (28, 29). Recently, we studied the epigenetic modification effect of RBM15 in tumor biology (18, 20). As an oncogene, RBM15 plays a vital role in laryngeal squamous cell carcinoma progression through the RBM15/IGF2BP3/TMBIM6 axis. RBM15-mediated m6A modification of TMBIM6 mRNA enhanced the stability of TMBIM6, which depends on the m6A reader IGF2BP3 (29). A previous study has shown that RBM15 and its paralogue RBM15B bind the m6A methylation complex to regulate the formation of XIST lncRNA m6A (30). Another study revealed that RBM15 is involved in the mechanism of mRNA methylation in the developing cortex (31).

In this study, we confirmed the interaction of RBM15 and circ-CTNNB1, which are both primarily localized in the nucleus. Upregulated circ-CTNNB1 exerted an oncogenic role in OS tumor progression in a RBM15-dependent manner. Mechanistically, circ-CTNNB1 binds RBM15 to perform the m6A modification of the key aerobic glycolysis genes HK2, GPI, and PGK1 and thus stabilize the mRNA levels of the target genes. Consistently, we observed a dynamic aerobic glycolysis process in OS cells (i.e., decrease and increase of the glucose uptake, lactate production, and ATP levels of OS cells for knockdown or overexpression of circ-CTNNB1, respectively). Then, the process of aerobic glycolysis ensures a survival advantage of tumor cells in the development and progression of cancer.

The excessive demand of tumors for nutrients is also associated with severe metabolic challenges. Through metabolic remodeling, tumors have evolved a unique metabolic regulation system (32, 33).

Therefore, tumors have also been viewed as metabolic disease (34–36). Aerobic glycolysis is the first discovered and most important event in the metabolic reprogramming process. Unlike normal cells obtain energy mainly from the aerobic oxidation of glucose, tumor cells prefer anaerobic glycolysis to maintain their growth and survival, even in the presence of sufficient oxygen, which is known as the “Warburg effect” (37, 38). This metabolic reprogramming not only provides ATP for tumor cells but also essential macromolecules for their protein and nucleotide biosynthesis (38). Subsequently, elevated glucose uptake and gluconeogenesis inhibition were also revealed in cancer cells. Moreover, both lipid and amino acid metabolism were abnormal in various cancers (33). All of the metabolic reprogramming process could be a promising treatment target. Therefore, our research provides a potential choice for OS therapy from the metabolic point of view.

The circ-CTNNB1/RBM15/aerobic glycolysis pathway could be intervened in different ways. CircRNAs are typically knocked down by RNA interference (RNAi)-based strategies. However, this is accompanied by many limitations, including their instability, lack of cell specificity, low intracellular entry, immune system activation, and other off-target effects (15, 39, 40). Using nanoparticles or exosomes as delivery systems can partly improve their efficacy (41, 42). On the one hand, CRISPR technology and Cas13 systems showed great potential in knocking down circRNAs in a specific and robust manner (43). On the other hand, disturbance of the interaction between circ-CTNNB1 and RBM15 with dominant-negative mutants or small molecular inhibitors are also relatively specific strategies. In our previous study, the growth and aggressiveness of various other cancer cells were efficiently suppressed by a cell-penetrating inhibitory peptide, which blocks the interaction of circ-CTNNB1 and that of the partner protein DDX3 (16). Therefore, we will further study a way to target this pathway and provide transformation value.

Conclusions

In summary, oncogenic circ-CTNNB1 is upregulated in OS tissues and cells. High circ-CTNNB1 expression was associated with a poor prognosis of OS patients and increased aggression of OS cells. Circ-CTNNB1 interacted with RBM15 to facilitate m6A modification of its aerobic glycolysis genes, resulting in more stable mRNA and activation of target genes. Moreover, the aerobic glycolysis level was elevated, which increased the survival advantage of OS cells. Our study provides a new theoretical basis to improve OS therapy.

Abbreviations

cDNA: Complementary DNA

circRNA: Circular RNA

ECAR: Extracellular acidification rate

EMSA: RNA electrophoretic mobility shift

FISH: Fluorescence in situ hybridization

gDNA: Genomic DNA

GPI: Glucose-6-phosphate isomerase

HK2: Hexokinase 2

m6A: N6-methyladenosine

OCR: Oxygen consumption rate

PGK1: Phosphoglycerate kinase 1

RIP: RNA immunoprecipitation

MS: Mass spectrometry

OS: Osteosarcoma

RBM15: RNA binding motif protein 15

SD: Standard deviation

shRNA: Short hairpin RNA

TF: Transcription factor

Declarations

Ethics approval and consent to participate

All human tissue studies were conducted in accordance with the ethical standards of the Ethics Committee of the First Affiliated Hospital of Nanchang University. All animal experiments were approved by the Animal Care Committee of Tongji Medical College, Huazhong University of Science and Technology.

Consent for publication

Written informed consent was obtained from all patients.

Availability of data and materials

The data supporting the conclusions of this article are included in this article and its additional files.

Competing interests

The authors declare that they have no competing interests.

Funding

This work was supported by the National Natural Science Foundation of China (82003127, 82103616, 82103339) and the Natural Science Foundation of Jiangxi Province (Grant No. 20181ACB20024)

Authors' contributions

Conception and design of the study were provided by F. Y. Most of the experiments were conceived and performed by H. L., J. X., and B. L.. Some of the in vitro experiments were accomplished by J. Z. and Y. C.. The in vivo studies were accomplished by A. H.. Y. L. and F. Y. wrote the manuscript and were responsible for its revision. The authors read and approved the final manuscript.

Acknowledgements

Not applicable.

References

1. Siegel RL, Miller KD, Fuchs HE, Jemal A. Cancer Statistics, 2021. CA: a cancer journal for clinicians. 2021;71(1):7-33.
2. Li Z, Shen J, Chan MT, Wu WK. MicroRNA-379 suppresses osteosarcoma progression by targeting PDK1. Journal of cellular and molecular medicine. 2017;21(2):315–23.
3. Xu R, Feng F, Yu X, Liu Z, Lao L. LncRNA SNHG4 promotes tumour growth by sponging miR-224-3p and predicts poor survival and recurrence in human osteosarcoma. Cell proliferation. 2018;51(6):e12515-e.
4. Yang C, Wu K, Wang S, Wei G. Long non-coding RNA XIST promotes osteosarcoma progression by targeting YAP via miR-195-5p. Journal of cellular biochemistry. 2018;119(7):5646–56.
5. Li Z, Li X, Xu D, Chen X, Li S, Zhang L, et al. An update on the roles of circular RNAs in osteosarcoma. Cell proliferation. 2021;54(1):e12936-e.
6. Kristensen LS, Andersen MS, Stagsted LVW, Ebbesen KK, Hansen TB, Kjems J. The biogenesis, biology and characterization of circular RNAs. Nature reviews Genetics. 2019;20(11):675–91.
7. Hanniford D, Ulloa-Morales A, Karz A, Berzoti-Coelho MG, Moubarak RS, Sánchez-Sendra B, et al. Epigenetic Silencing of CDR1as Drives IGF2BP3-Mediated Melanoma Invasion and Metastasis. Cancer cell. 2020;37(1):55-70.e15.
8. Huang A, Zheng H, Wu Z, Chen M, Huang Y. Circular RNA-protein interactions: functions, mechanisms, and identification. Theranostics. 2020;10(8):3503–17.
9. Lei M, Zheng G, Ning Q, Zheng J, Dong D. Translation and functional roles of circular RNAs in human cancer. Molecular cancer. 2020;19(1):30.

10. Yang F, Hu A, Guo Y, Wang J, Li D, Wang X, et al. p113 isoform encoded by CUX1 circular RNA drives tumor progression via facilitating ZRF1/BRD4 transactivation. Molecular cancer. 2021;20(1):123.
11. Li J, Sun D, Pu W, Wang J, Peng Y. Circular RNAs in Cancer: Biogenesis, Function, and Clinical Significance. Trends in cancer. 2020;6(4):319–36.
12. Wu J, Qi X, Liu L, Hu X, Liu J, Yang J, et al. Emerging Epigenetic Regulation of Circular RNAs in Human Cancer. Molecular therapy Nucleic acids. 2019;16:589–96.
13. Wang X, Li H, Lu Y, Cheng L. Regulatory Effects of Circular RNAs on Host Genes in Human Cancer. Frontiers in oncology. 2020;10:586163.
14. Zhang Z, Yang T, Xiao J. Circular RNAs: Promising Biomarkers for Human Diseases. EBioMedicine. 2018;34:267–74.
15. He AT, Liu J, Li F, Yang BB. Targeting circular RNAs as a therapeutic approach: current strategies and challenges. Signal transduction and targeted therapy. 2021;6(1):185.
16. Yang F, Fang E, Mei H, Chen Y, Li H, Li D, et al. Cis-Acting circ-CTNNB1 Promotes β-Catenin Signaling and Cancer Progression via DDX3-Mediated Transactivation of YY1. Cancer research. 2019;79(3):557–71.
17. Deng X, Su R, Feng X, Wei M, Chen J. Role of N(6)-methyladenosine modification in cancer. Current opinion in genetics & development. 2018;48:1–7.
18. Wang T, Kong S, Tao M, Ju S. The potential role of RNA N6-methyladenosine in Cancer progression. Molecular cancer. 2020;19(1):88.
19. Wang M, Yang Y, Yang J, Yang J, Han S. circ_KIAA1429 accelerates hepatocellular carcinoma advancement through the mechanism of m(6)A-YTHDF3-Zeb1. Life sciences. 2020;257:118082.
20. Jiang X, Liu B, Nie Z, Duan L, Xiong Q, Jin Z, et al. The role of m6A modification in the biological functions and diseases. Signal transduction and targeted therapy. 2021;6(1):74.
21. Chi F, Cao Y, Chen Y. Analysis and Validation of circRNA-miRNA Network in Regulating m(6)A RNA Methylation Modulators Reveals CircMAP2K4/miR-139-5p/YTHDF1 Axis Involving the Proliferation of Hepatocellular Carcinoma. Frontiers in oncology. 2021;11:560506.
22. Li H, Yang F, Hu A, Wang X, Fang E, Chen Y, et al. Therapeutic targeting of circ-CUX1/EWSR1/MAZ axis inhibits glycolysis and neuroblastoma progression. EMBO molecular medicine. 2019;11(12):e10835.
23. Chen Y, Yang F, Fang E, Xiao W, Mei H, Li H, et al. Circular RNA circAGO2 drives cancer progression through facilitating HuR-repressed functions of AGO2-miRNA complexes. Cell death and differentiation. 2019;26(7):1346–64.
24. Li D, Song H, Mei H, Fang E, Wang X, Yang F, et al. Armadillo repeat containing 12 promotes neuroblastoma progression through interaction with retinoblastoma binding protein 4. Nature communications. 2018;9(1):2829.
25. Wang X, Ma R, Zhang X, Cui L, Ding Y, Shi W, et al. Crosstalk between N6-methyladenosine modification and circular RNAs: current understanding and future directions. Molecular cancer.

2021;20(1):121.
26. Lei K, Bai H, Wei Z, Xie C, Wang J, Li J, et al. The mechanism and function of circular RNAs in human diseases. Experimental cell research. 2018;368(2):147–58.
27. Yang F, Hu A, Li D, Wang J, Guo Y, Liu Y, et al. Circ-HuR suppresses HuR expression and gastric cancer progression by inhibiting CNBP transactivation. Molecular cancer. 2019;18(1):158-.
28. Hiriart E, Gruffat H, Buisson M, Mikaelian I, Keppler S, Meresse P, et al. Interaction of the Epstein-Barr virus mRNA export factor EB2 with human Spen proteins SHARP, OTT1, and a novel member of the family, OTT3, links Spen proteins with splicing regulation and mRNA export. The Journal of biological chemistry. 2005;280(44):36935–45.
29. Wang X, Tian L, Li Y, Wang J, Yan B, Yang L, et al. RBM15 facilitates laryngeal squamous cell carcinoma progression by regulating TMBIM6 stability through IGF2BP3 dependent. Journal of experimental & clinical cancer research: CR. 2021;40(1):80.
30. Patil DP, Chen CK, Pickering BF, Chow A, Jackson C, Guttman M, et al. m(6)A RNA methylation promotes XIST-mediated transcriptional repression. Nature. 2016;537(7620):369–73.
31. Xie Y, Castro-Hernandez R, Sokpor G, Pham L, Narayanan R, Rosenbusch J, et al. RBM15 Modulates the Function of Chromatin Remodeling Factor BAF155 Through RNA Methylation in Developing Cortex. Molecular neurobiology. 2019;56(11):7305–20.
32. Hanahan D, Weinberg RA. Hallmarks of cancer: the next generation. Cell. 2011;144(5):646–74.
33. Pavlova NN, Thompson CB. The Emerging Hallmarks of Cancer Metabolism. Cell metabolism. 2016;23(1):27–47.
34. Seyfried TN, Shelton LM. Cancer as a metabolic disease. Nutrition & metabolism. 2010;7:7.
35. Seyfried TN, Flores RE, Poff AM, D'Agostino DP. Cancer as a metabolic disease: implications for novel therapeutics. Carcinogenesis. 2014;35(3):515–27.
36. Wishart DS. Is Cancer a Genetic Disease or a Metabolic Disease? EBioMedicine. 2015;2(6):478–9.
37. Warburg O. On respiratory impairment in cancer cells. Science (New York, NY). 1956;124(3215):269–70.
38. Zhang X, Zhao H, Li Y, Xia D, Yang L, Ma Y, et al. The role of YAP/TAZ activity in cancer metabolic reprogramming. Molecular cancer. 2018;17(1):134.
39. Singh S, Narang AS, Mahato RI. Subcellular fate and off-target effects of siRNA, shRNA, and miRNA. Pharmaceutical research. 2011;28(12):2996–3015.
40. Robbins M, Judge A, MacLachlan I. siRNA and innate immunity. Oligonucleotides. 2009;19(2):89–102.
41. Kulkarni JA, Witzigmann D, Chen S, Cullis PR, van der Meel R. Lipid Nanoparticle Technology for Clinical Translation of siRNA Therapeutics. Accounts of chemical research. 2019;52(9):2435–44.
42. Williford JM, Wu J, Ren Y, Archang MM, Leong KW, Mao HQ. Recent advances in nanoparticle-mediated siRNA delivery. Annual review of biomedical engineering. 2014;16:347–70.

43. Li S, Li X, Xue W, Zhang L, Yang L-Z, Cao S-M, et al. Screening for functional circular RNAs using the CRISPR-Cas13 system. Nature methods. 2021;18(1):51–9.

Figures

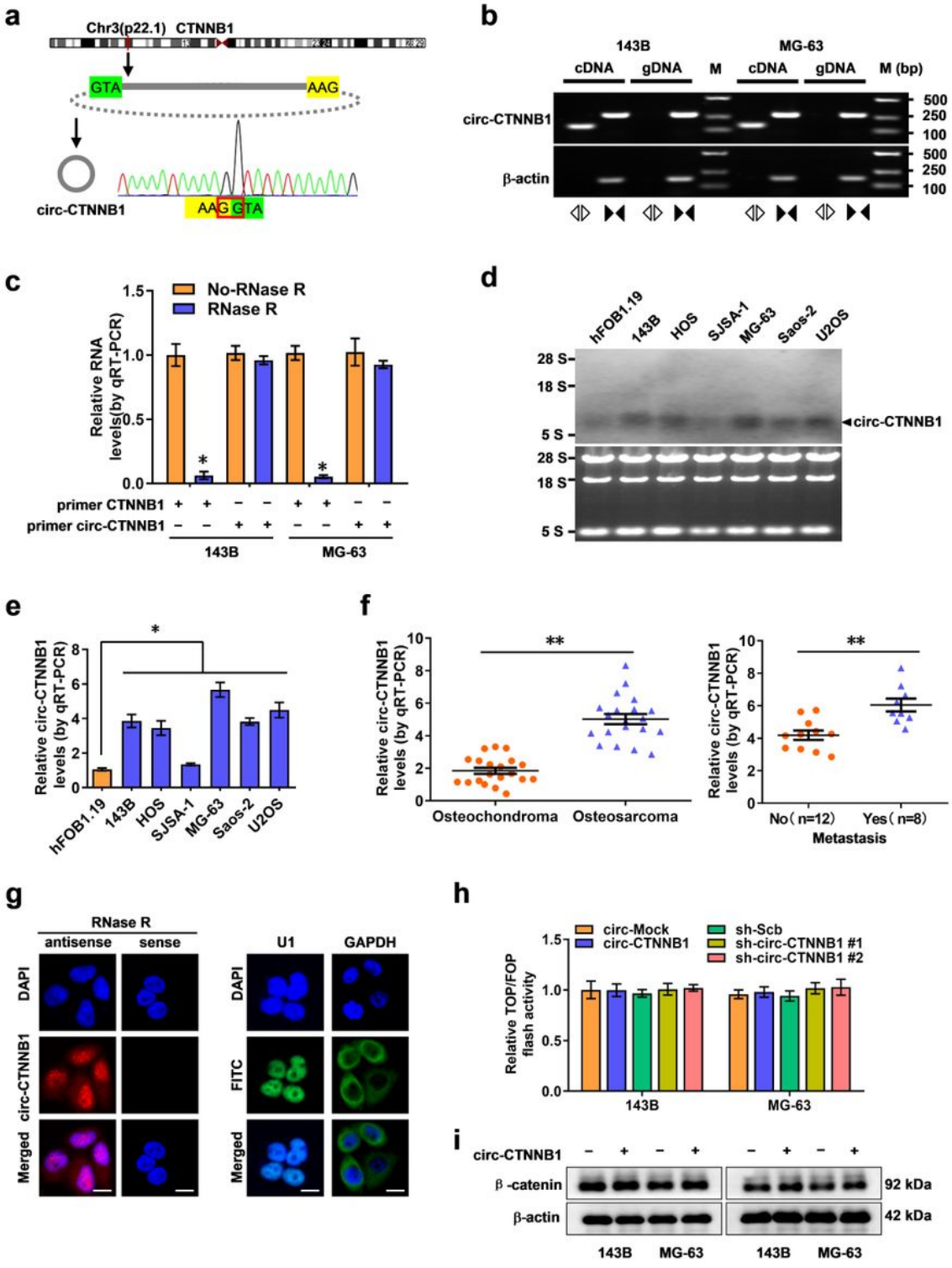

Figure 1

Expression of circ-CTNNB1 in OS cell lines and tissues, and subcellular location of circ-CTNNB1. a Schematic illustration of the genomic location of circ-CTNNB1 derived from its host gene and validation by Sanger sequencing. b RT-PCR assay showing the presence of circ-CTNNB1 with divergent and convergent primers from cDNA or genomic DNA (gDNA) of differential OS cell lines using β-actin as the negative control. c qRT-PCR analysis of the expression of circ-CTNNB1 after RNase R treatment in 143B or MG-63 cells. d Northern blot showing the differential expression of circ-CTNNB1 in hFOB 1.19 cells and OS cell lines. e & f qRT-PCR assay showing the relative levels of circ-CTNNB1 (normalized to β-actin) in cultured cell lines and human tissues. g RNA-FISH assay showing the nuclear localization of hsa_circ_0049027 in AGS cells with an antisense probe (green), and the sense probe was used as a negative control. Nuclei were stained with DAPI (blue), and U1 and GAPDH were used as positive controls. Scale bar: 10 μm. h & i TOP/FOP flash assay (h) and Western blot (i) assay revealing the β-catenin activity and protein levels of CTNNB1 in 143B and MG-63 cells. (Data were mean ± SEM of three experiments. Student's t test and ANOVA compared the difference in c, e, f, h. *P<0.05, **P<0.01).

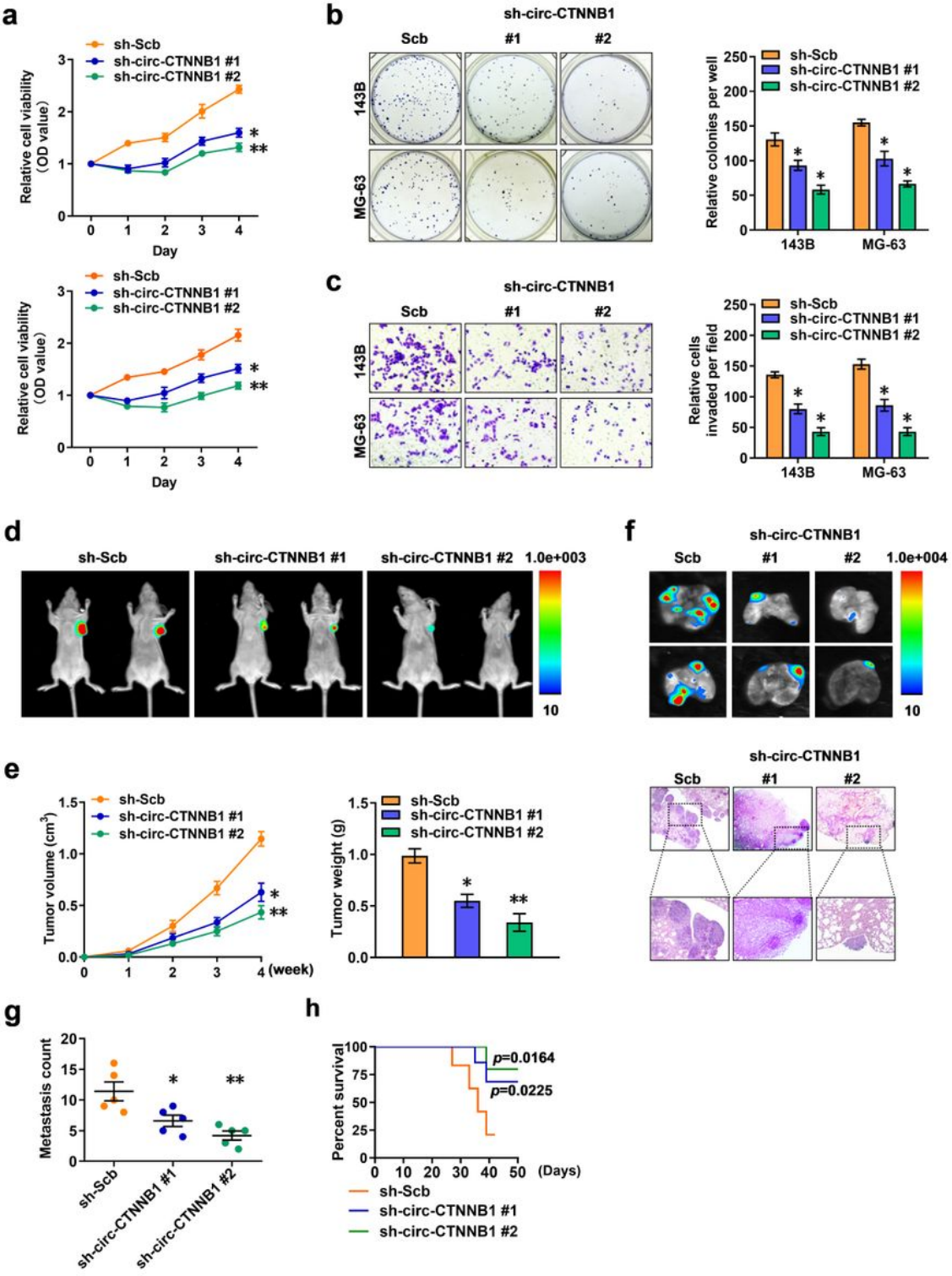

Figure 2

Knockdown of circ-CTNNB1 inhibits the growth and aggressiveness of OS in vitro and in vivo. a MTT assay of 143B and MG-63 cells stably transfected with scrambled shRNA (sh-Scb) and sh-circ-CTNNB1#1, #2. b & c In vitro growth and invasion of 143B and MG-63 cells stably transfected with sh-Scb and sh-circ-CTNNB1#1, #2, as revealed by colony formation (b) and matrigel invasion (c) assays. d & e MG-63 cells with stable expression of sh-Scb and sh-circ-CTNNB1#1, #2 were injected into the dorsal

flanks of nude mice (n=5 for each group). In vivo growth curve and weight measured at the end point of the xenografts. f-h MG-63 cells stably transfected with sh-Scb and sh-circ-CTNNB1#1, #2 were injected into the tail vein of nude mice (n=5 for each group). Representative images of HE staining (f), quantification of lung metastatic colonization (g), and collected Kaplan-Meier curves (h). (Data were mean ± SEM of three experiments. ANOVA analyzed the difference in a-c, e, g. Log-rank test for survival comparison in h. *P < 0.05 vs. sh-Scb, **P < 0.01 vs. sh-Scb).

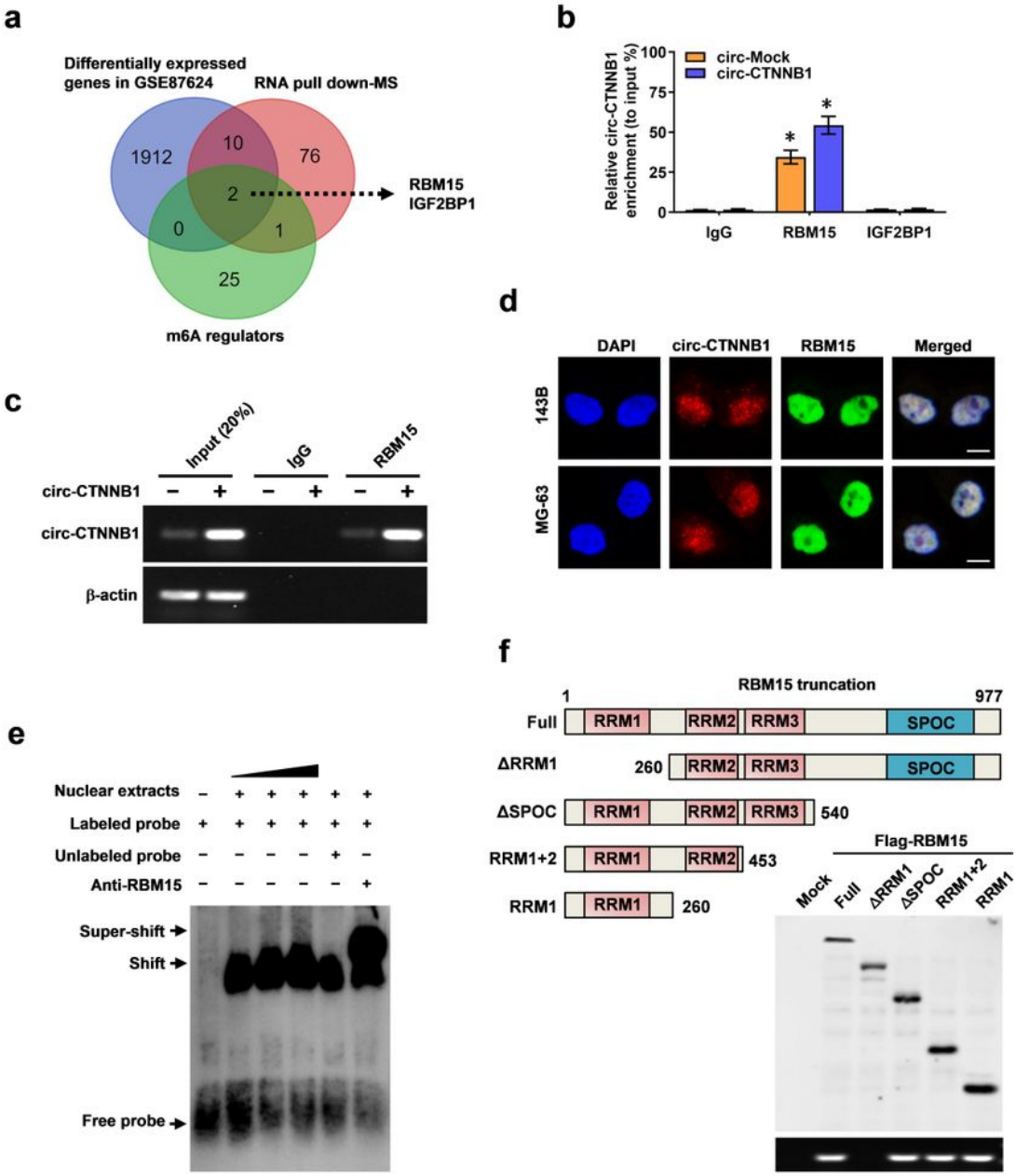

Figure 3

Screening of protein interactions with circ-CTNNB1. a Overlapping analysis (Venn diagram) revealing the m6A regulators that were pulled down by biotin-labeled circ-CTNNB1 from the lysates of MG-63 cells in mass spectrometry (MS) assays with differentially expressed genes in OS cells (GSE87624) and m6A regulators. b RIP and qRT-PCR assays showing the interaction between circ-CTNNB1 and two proteins in OS cells. c RIP assays revealing the interaction between circ-CTNNB1 and RBM15 in MG-63 cells stably transfected with circ-Mock or circ-CTNNB1. d Dual RNA FISH and immunofluorescence staining assays showing the colocalization of circ-CTNNB1 (red) and RBM15 (green) in cultured 143B and MG-63 cells with DAPI nuclei staining (blue). Scale bar: 10 μm. e RNA EMSA showing the interaction between endogenous RBM15 and biotin-labeled RNA probe for circ-CTNNB1 (arrowheads), with RBM15 antibody or competition using an excess of unlabeled homologous circ-CTNNB1 probe. f Schematic diagram showing the domains of RBM15 truncations (upper panel), and in vitro binding assay (lower panel) showing the enriched circ-CTNNB1 levels detected by RT-PCR after incubation with full-length or truncated forms of FLAG-tagged recombinant RBM15 protein validated by Western blot. (Data were mean ± SEM of three experiments. Fisher's exact test for over-lapping analysis in a, ANOVA analyzed the difference in b. *P < 0.05 vs. IgG).

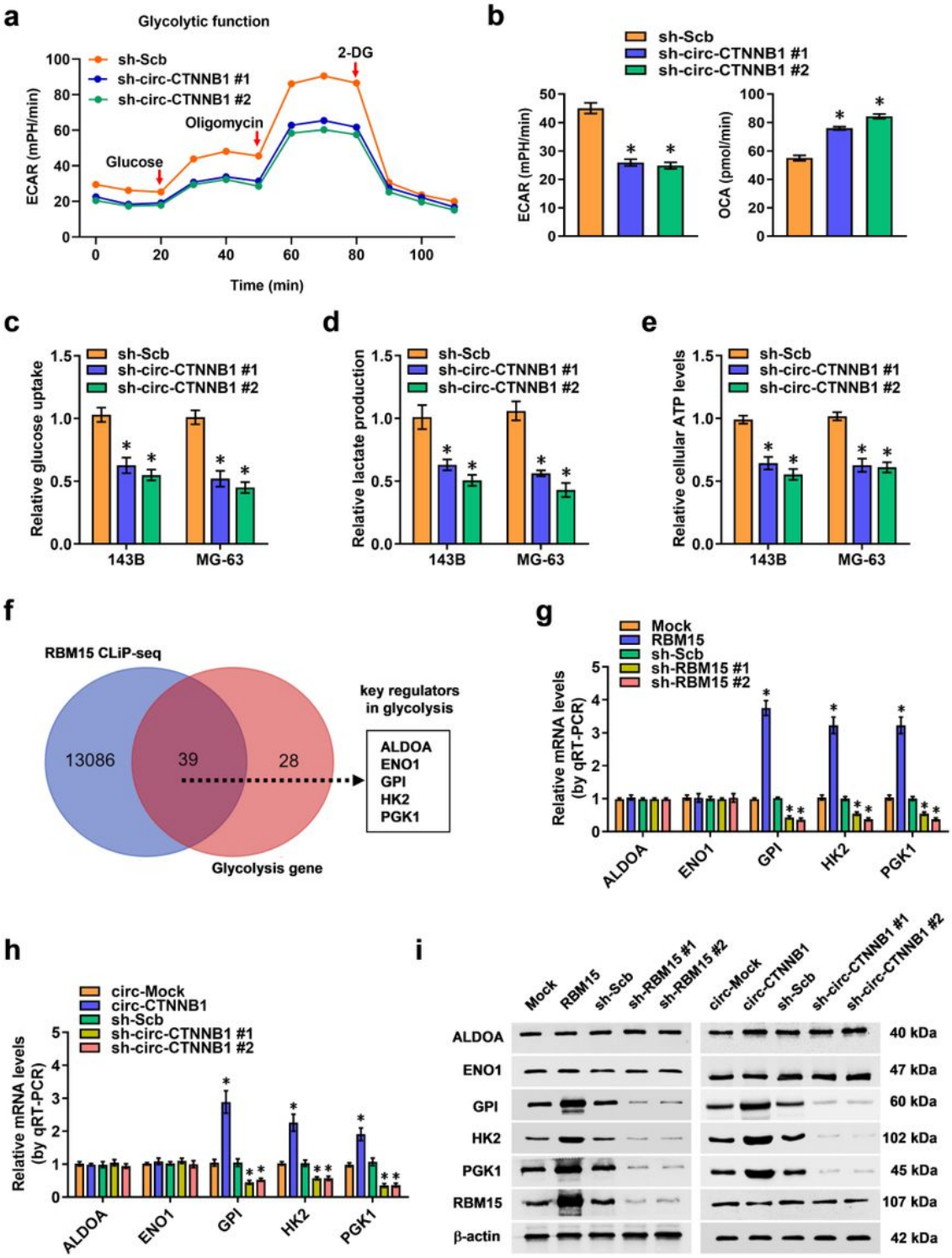

Figure 4

Circ-CTNNB1 promotes aerobic glycolysis in OS. a & b Seahorse tracing curves (a) and ECAR and OCR (b) of MG-63 cells stably transfected with sh-Scb and sh-circ-CTNNB1#1, #2 or treated with glucose (10 mM), oligomycin (2 μM), or 2-deoxyglucose (2-DG, 50 mM) at indicated points. c-e Glucose uptake (c), lactate production (d), and ATP levels (e) in 143B and MG-63 cells stably transfected with sh-Scb and sh-circ-CTNNB1#1, #2. f Venn diagram overlapping RBM15 CLIP-seq with glycolytic genes revealing five target

genes involved in the aerobic glycolysis of the circ-CTNNB1/RBM15 axis. g-i Transcript and protein expression levels of ALDOA, ENO1, GPI, HK2, and PGK1 in MG-63 cells with overexpression or knockdown of RBM15 and circ-CTNNB1 measured by qRT-PCR (g, h) and Western blot (i) assay. (Data were mean ± SEM of three experiments. Fisher's exact test for over-lapping analysis in f, Student's t test and ANOVA analyzed the difference in a-e, g, h. *P < 0.05 vs. sh-Scb, mock or circ-Mock).

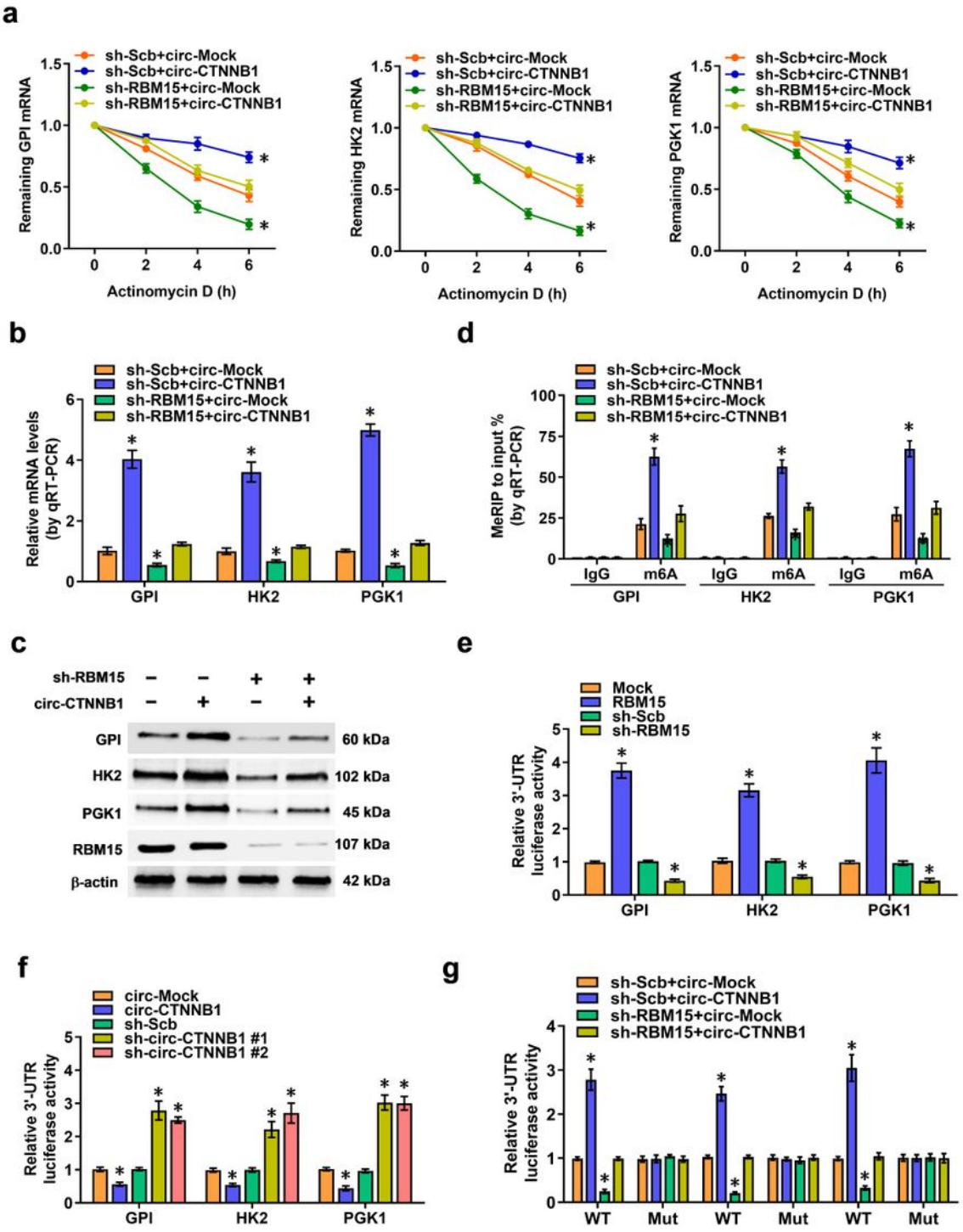

Figure 5

Circ-CTNNB1 facilitates RBM15-mediated gene activation via m6A regulation. a qRT-PCR assay indicating the half-life levels of GPI, HK2, and PGK1 mRNA (normalized to β-actin) in MG-63 cells treated with actinomycin D (1 μg/mL) for the indicated periods of time and stably transfected with sh-Scb or sh-RBM15 or co-transfected with circ-Mock or circ-CTNNB1. b & c qRT-PCR (b) and Western blot (c) assays revealing the transcript and protein expression levels of GPI, HK2, and PGK1 mRNA (normalized to β-actin) in MG-63 cells stably transfected with sh-Scb or sh-RBM15 or co-transfected with circ-Mock or circ-CTNNB1. d MeRIP-qPCR assay followed by qRT-PCR revealing the GPI, HK2, and PGK1 m6A modification in MG-63 cells stably transfected with sh-Scb or sh-RBM15 or co-transfected with circ-Mock or circ-CTNNB1. e & f Dual-luciferase assay revealing the 3'-UTR activity of GPI, HK2, and PGK1 in OS cells stably transfected with overexpression or knockdown of RBM15 or circ-CTNNB1. g Wild-type or m6A site mutation of 3'-UTR was established, and dual-luciferase assay revealed the 3'-UTR activity of GPI, HK2, and PGK1 in OS cells stably transfected with sh-Scb or sh-RBM15 or co-transfected with circ-Mock or circ-CTNNB1. (Data were mean ± SEM of three experiments. Student's t test and ANOVA analyzed the difference in a, b, d-g. *P < 0.05 vs. sh-Scb+circ-Mock, mock, circ-Mock, sh-Scb).

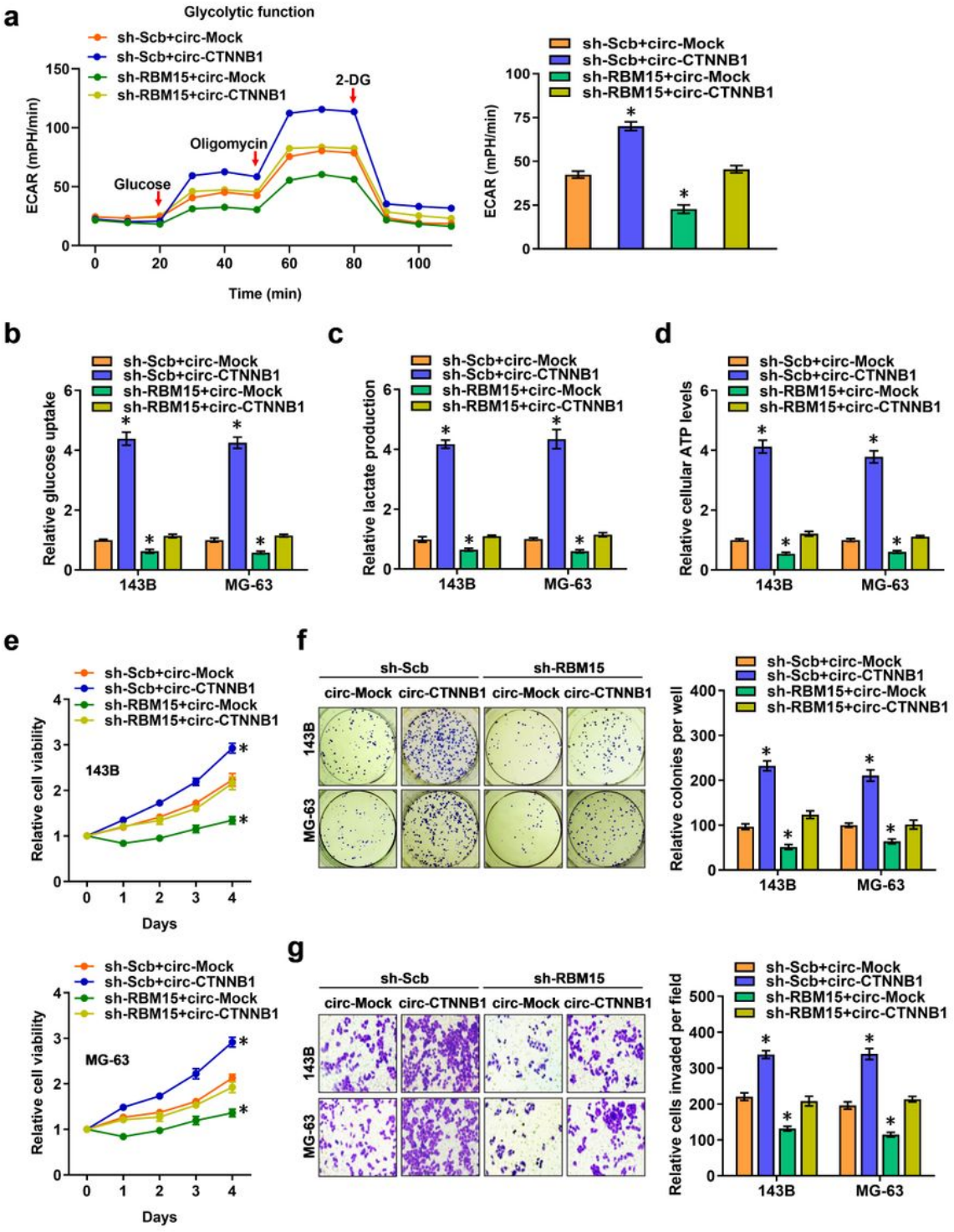

Figure 6

Circ-CTNNB1 promotes aerobic glycolysis and OS progression by interacting with RBM15. a Seahorse tracing curves (left) and ECAR (right) of MG-63 cells treated with glucose (10 mM), oligomycin (2 μM), or 2-deoxyglucose (2-DG, 50 mM) at indicated points and stably transfected with sh-Scb or sh-RBM15 or co-transfected with circ-Mock or circ-CTNNB1. b-d Glucose uptake (b), lactate production (c), and ATP levels (d) in 143B and MG-63 cells stably transfected with sh-Scb or sh-RBM15 or co-transfected with circ-Mock

or circ-CTNNB1. e MTT assay showing the vitality of 143B and MG-63 cells stably transfected with sh-Scb or sh-RBM15 or co-transfected with circ-Mock or circ-CTNNB1. f & g In vitro growth and invasion of 143B and MG-63 cells stably transfected with sh-Scb or sh-RBM15 or co-transfected with circ-Mock or circ-CTNNB1, as revealed by colony formation (f) and matrigel invasion (g) assay (Data were mean ± SEM of three experiments. Student's t test and ANOVA analyzed the difference in a-g. *P<0.05 vs. sh-Scb+circ-Mock).

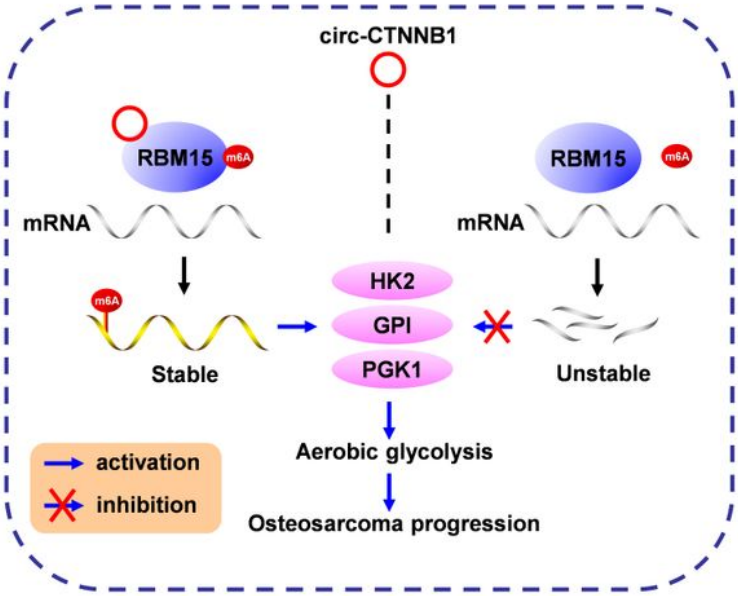

Figure 7

Mechanisms underlying circ-CTNNB1-promoted OS progression.

Supplementary Files

This is a list of supplementary files associated with this preprint. Click to download.

- Additionalfile1TableS1.doc
- Additionalfile1TableS2.doc
- Additionalfile1TableS3.xlsx
- Additionalfile2FigureS1.jpg
- Additionalfile2FigureS2.jpg
- Additionalfile2FigureS3.jpg